Scientia Iranica F (2021) 28(3), 1896–1907

SCIENTIA IRANICA

Sharif University of Technology
Scientia Iranica
*Transactions F: Nanotechnology*
http://scientiairanica.sharif.edu

# Bioconvection phenomenon for the boundary layer flow of magnetohydrodynamic Carreau liquid over a heated disk

**M. Sohail[a], U. Nazir[a], Y.-M. Chu[b,c,*], W. Al-Kouz[d], and P. Thounthong[e]**

a. *Department of Applied Mathematics & Statistics, Institute of Space Technology Islamabad, P.O. Box 2750, Pakistan.*
b. *Department of Mathematics, Huzhou University, Huzhou 313000, P. R. China.*
c. *Hunan Provincial Key Laboratory of Mathematical Modeling and Analysis in Engineering, Changsha University of Science & Technology, Changsha 410114, P. R. China.*
d. *Department of Mechanical Engineering, College of Engineering, Prince Muhammad bin Fahd University, Al-Khobar, Saudi Arabia.*
e. *Renewable Energy Research Centre, Department of Teacher Training in Electrical Engineering, Faculty of Technical Education, King Mongkut's University of Technology North Bangkok, 1518 Pracharat 1 Road, Bangsue, Bangkok 10800, Thailand.*

Received 8 July 2019; received in revised form 25 October 2020; accepted 26 April 2021

**KEYWORDS**
Brownian diffusion;
Heat and mass transport;
Carreau fluid;
Bioconvective process;
Rotating heated disk;
Boundary layer analysis.

**Abstract.** This study carried out a numerical examination on the effect of magnetohydrodynamic steady flow of Carreau fluid on the transfer of thermal energy and mass species comprising nanoparticles with gyrotactic microorganisms through a heated disk. The roles of thermophoresis and Brownian motion were also considered in resolving this flow problem. Governing equations were solved using boundary layer theory emphasizing the coupled system of Partial Differential Equations (PDEs) involving boundary conditions. The highly non-linear system of Ordinary Differential Equations (ODEs) was generated using transformation approach. Due to the highly nonlinear form of the system of transformed equations, an approximate solution was presented which was evaluated using optimal homotopy method. Moreover, the effects of prominent parameters on velocity, thermal energy, mass species, and motile density microorganisms were graphically examined. In addition, graphical observations regarding the mass species, thermal energy, and velocities were briefly discussed. It was estimated that in an intensified magnetic field, the motion of fluid particles and temperature of fluid would decrease and increase, respectively.



## 1. Introduction

Due to their extensive applicability, non-Newtonian fluids have drawn much academic attention. This research is motivated by the abundance of these fluids in nature, as well. Such fluids are widely used in different fields such as foodstuffs, extrusion of molten polymers and plastics, fiber synthesis, drilling gas and oil wells, etc. Many studies have been conducted on non-Newtonian fluids and their phenomenal roles. For instance, a number of researchers have investigated how to improve the thermal conductivity of non-Newtonian liquids. In addition, some others have shifted their focus to the difference in modeling the power law for non-Newtonian fluids. However, the power law model suffers some drawbacks including low and high shear rates and then, authors have examined the viscosity

*. *Corresponding author. Tel.: +86-572-2322189*
*E-mail address: chuyuming@zjhu.edu.cn (Y.-M. Chu)*

doi: 10.24200/sci.2021.53970.3518

model called Carreau rheology. This is a special type of Newtonian liquid and the shear rate is a function of viscosity; this phenomenon is useful for high shear-rate liquids. Carreau [1,2] employed an important theory regarding rheological equations based on network molecular models. Griffiths [3] studied the flow behavior of generalized Newtonian liquid through disk by applying the Carreau fluid model. Machireddy and Naramgari [4] discussed the role of transfer of thermal energy and mass species with cross-diffusion involving Magnetohydrodynamic (MHD) Carreau fluid on the stretch surface. Another notable study on Carreau fluid can be found in [5–8] with various explorations therein. Nanoparticles are tiny particles made of dense nanoparticles or nanofibers ranging between (1-100 nm) which are normally equated through the conventional heat carrying fluids, and they enjoy an advanced thermal conductivity. As can be found in the literature, Choi and Eastman [9] initially put forward the idea of utilizing fluid consisting of nano-sized particles and base fluid, called nanofluid. There are many applications containing insulation of energy, astronomical, cooling processes, solar amusement and defense, magnetic sticking, mass/heat transport strengthening and medical instruments, etc. Such applications require substantial point altering from conventional fluids. Therefore, the current authors of this study have become drawn to nanofluid and discussed some useful findings which were previously extracted from Refs. [10–15].

MHD is an added working zone of building sciences nowadays that includes the effect of magnetic fields. Applications of such types of fluid flow are pumps, power generators, magnetic drug treatment, accelerators, plasma studies, and flow meters. Bhatti et al. [16] discussed mathematical modeling of mass and heat effects on the flow of electrically conducting fluid for two-phase peristaltic propulsion through a porous medium with Darcy-Brinkman-Forchheimer. Many researchers [17–20] interpreted different aspects of non-Newtonian fluid such as Williamson, Micropolar and Carreau fluids, etc.

Heat forms out of energy and is transmitted from one place to another, the difference of which may turn into thermal energy. Physics can help read the investigations to produce the energy difference called heat transfer. The mathematical form of heat transfer is derived from Fourier's law of conduction. For heat transfer measurement, thermal conductivity is a very important factor which is defined as the ability to measure heat conduction. The enhancement of thermal conductivity for a material is suggestive of being a good conductor while a poor insulator results from low thermal conductivity. Similarly, transport of mass species involves the movement or diffusion of fluid particles from one place to another. Transport of thermal energy and mass species are the kinetic processes that may be investigated, either separately or jointly. The transport of thermal energy and solubility of nanofluid can be investigated based on Fick's and Fourier's laws. These movements are modeled by similar mathematical equations in the form of convection and diffusion and both transfer types must be considered jointly in some cases, i.e., ablation and evaporative cooling. Applications of mass species and thermal energy transport in different fields including oil transport wonder, dispersion of specific medications in blood, food preparation, cooling of electronic equipment, manufacturing/materials processing, absorption, drying, precipitation, membrane filtration, and evaporation can be seen in [21]. For further information on mass and heat transfer applications, readers are referred to [22–24] and the studies cited therein for further insights.

Rotation is the most powerful and useful tool for such as applications medical equipment, gas turbine, food processing, and computer operating, while numerous other applications have been found in food of rotating geometries (disk, cylinder, and surface). It is evident that rotating disk has an important role from the research viewpoint. Concept of rotating disk was developed by Karman first [25]. He employed transformation (Von-Karmaan) to evaluate solution flow problems over heated rotating disk. Several other applications for rotations can be found in [26–28].

The particles of this impact (bio-convection) which are not self-boosted microorganisms have been investigated. Another terminology for the bio-convection approach is called boosted microorganism. So, this type of terminology was initiated by Platt [29] who concluded that drag force could be generated from the movement of microorganisms while gravitation torque was produced due to the equilibrium position of particles in the cells of swimming microorganism. Chakraborty et al. [30] explored the remaining unknown aspects of the magnetic field and nanoparticles with emphasis on gyrotactic microorganisms. Impact between gyrotactic microorganisms and nanoparticles and the resulting radiation were measured by Khan et al. [31]. For deeper insights, readers are referred to the works mentioned in [32–34] and other references therein.

Satisfactory performance of a solution should be taken into consideration from two aspects: the case of approximate solution and generation of an accurate approximate solution with different parameters. Numerous approaches are employed to find a solution to linear flow problems. In the case of analytical technique, an analysis approach (Optimal Homotopy Analysis Method (OHAM)) captures a solution to non-linear flow problems involving Boundary Conditions (BCs). Recently, the OHAM approach has been adopted by Marinca et al. [35], with few relevant studies on algorithm being accessible in [36–39]. Makinde and Animasaun [40] proposed a new bouncy induced procedure for nanoparticles and considered volume fraction by causing variations in thermal conductivity for this flow problem while solving the flow problem by the (RK4SM) approach. Makinde and Animasaun [41] investigated the phenomenon of flow in terms of Brownian motion, bouncy force, and bio-convection through parabolic surface with microorganisms. Mutuku and Makinde [42] discussed the characteristics of bio-convection subject to hydro-magnetics considering nanoparticles. Khan et al. [43] explored lesser known aspects of gyrotactic microorganisms with nanoparticles and their impact on the transport of mass species and heat energy in the magnetic field. Makinde et al. [44] developed a flow model upon taking into account the influence of radiations, chemical reaction, Brownian motion, and magnetic force over vertical plate. The latest important contributions dealing with the flow problems were made and reported in [45–47].

This paper aims to delve into the phenomenon of flow emphasizing electrical conducting of Carreau rheological fluid with nanoparticles and gyrostatic microorganisms through heated cones. The system of Ordinary Differential Equations (ODEs) was derived from the system of Partial Differential Equations (PDEs) using Von-Karman transformations and the approach of OHAM analysis. This study is structured as follows: after presented a literature review, the mathematical formulation is developed in Section 2. The formulation of flow problem and numerical solution are captured in Sections 3 and 4, respectively. The key points regarding flow problem are added in Section 5. In the end, references are listed.

## 2. Mathematical formulation and fluid rheology

In this analysis, we have considered the flow of electrically conducting fluids including two-dimensional time-independent incompressible Carreau fluid and nanoparticles with motile gyrotactic microorganisms, as induced by a rotating disk. The magnetic field strength ($B_0$) on a boundary layer acts along the z-direction, while the motion of fluid particles is generated by the movement of wall velocity $u_s(= rl_0)$ where ($l_0$) is a constant. Geometrical flow under the current assumption is captured and given in Figure 1. The effect of induced magnetic field is not taken into account, but the features of thermophoresis and ambient motion are observed. The angular velocity ($\Omega_1$) represents the rotational velocity of a rotating disk involving viscous dissipation. The velocity components are based on directions of $(r, \theta, z)$. Initially, a disk is heated at ($T_0$) temperature, after which it adapts to

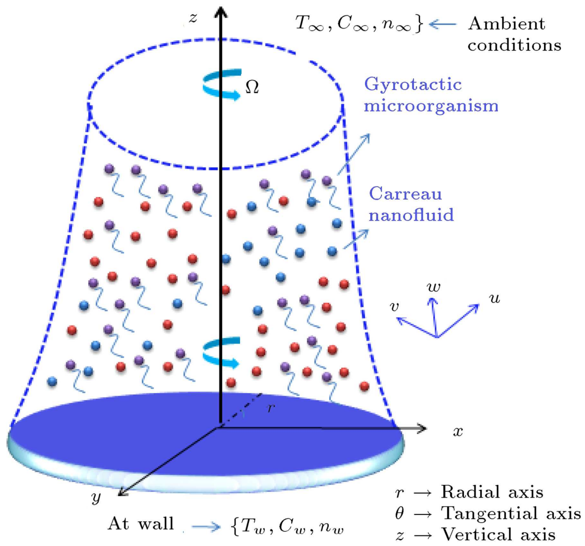


**Figure 1.** Fluid flow geometry.

and takes ambient temperature ($T_\infty$). Bio-convective patterns are detected based on the movement of motile microorganisms from higher areas to lower regions. The concentrations of reference and ambient microorganisms are taken by $n_0$ and $n_\infty$, respectively. The stress tensor [1] is expressed as follows:

$$\tau_1 = \left[\eta_0\left(1 + \lambda^2\dot{\gamma}^2\right)^{\frac{n-1}{2}}\right]\dot{\gamma}, \tag{1}$$

$$\dot{\gamma} = \left(\frac{1}{2}\sum_i\sum_j(\gamma_{ji}\gamma_{ij})\right)^{1/2}, \tag{2}$$

where $n$ is the power law index. It was estimated that Carreau rheology would become $(0 < n < 1)$ shear thinning and $(n > 1)$ shear thickening. Governing laws under motile microorganism and nanomaterial are handled in the following equations:

$$\nabla \cdot V = 0,$$

$$\rho_f[V \cdot \nabla]V = -\nabla P + \nabla \cdot \tau_1 + J_1 \times B,$$

$$J_1 = \sigma(V \times B),$$

$$B = [0,\, 0,\, B_0],$$

$$V\cdot\nabla T - \alpha^*\nabla^2 T = \tau\left[D_b\nabla T\cdot\nabla C + \left(\frac{D_t}{T_\infty}\right)\nabla T\cdot\nabla T\right],$$

$$(V\cdot\nabla)\, C = D_b\left(\nabla^2 C\right) + D_b\left(\nabla^2 C\right) + \left(\frac{D_t}{T_\infty}\right)\nabla^2 T,$$

$$\nabla \cdot J^* = 0,$$

where $V$ is velocity. $u_1, v_1, w_1$ are flow components; $P$ is pressure; $\rho_f$ is fluid density; $T$ is temperature; $\alpha^*$ is thermal diffusivity, $C$ is concentration, $D_t, D_b$ are thermophoretic diffusion and Brownian numbers; and $J^*$ is microorganisms flux.

$$J^* = nV + n \cdot \hat{V} - D_m \nabla n,$$

$$\hat{V} = \left(\frac{bW_c}{\Delta C}\right) \nabla C.$$

The above equations after the boundary layer approximations are expressed as follows:

$$\frac{\partial u_1}{\partial r} + \frac{u_1}{r} + \frac{\partial w_1}{\partial z} = 0, \tag{3}$$

$$\rho_f \left(u_1 \frac{\partial u_1}{\partial r} - \frac{v_1^2}{r} + w_1 \frac{\partial u_1}{\partial z}\right) = -\frac{\partial p}{\partial r} + \frac{\partial^2 u_1}{\partial z^2}\eta_0$$
$$\left[\begin{array}{c} 1+\frac{(n-1)}{2}\lambda^2 \left\{\left(\frac{\partial v_1}{\partial z}\right)^2 + \left(\frac{\partial u_1}{\partial z}\right)^2\right\} + \frac{(n-1)\,\lambda^4 (n-3)}{4(2)} \\ \left\{\left(\frac{\partial v_1}{\partial z}\right)^4 + \left(\frac{\partial u_1}{\partial z}\right)^4 + 2\left(\frac{\partial v_1}{\partial z}\frac{\partial u_1}{\partial z}\right)^2\right\} \end{array}\right]$$
$$+\eta \frac{\partial u_1}{\partial z}\frac{\partial}{\partial z}$$
$$\left[\begin{array}{c} \frac{(n-1)}{2}\lambda^2 \left\{\left(\frac{\partial v_1}{\partial z}\right)^2 + \left(\frac{\partial u_1}{\partial z}\right)^2\right\} + \frac{(n-1)\,\lambda^4 (n-3)}{4(2)} \\ \left\{\left(\frac{\partial v_1}{\partial z}\right)^4 + \left(\frac{\partial u_1}{\partial z}\right)^4 + 2\left(\frac{\partial v_1}{\partial z}\frac{\partial u_1}{\partial z}\right)^2\right\} \end{array}\right]$$
$$-\sigma B_0^2 u_1, \tag{4}$$

$$\rho_f \left(u_1 \frac{\partial v_1}{\partial r} - \frac{u_1 . v_1}{r} + w_1 \frac{\partial v_1}{\partial z}\right) = \frac{\partial^2 v_1}{\partial z^2}\eta_0$$
$$\left[\begin{array}{c} 1+\frac{(n-1)}{2}\lambda^2 \left\{\left(\frac{\partial v_1}{\partial z}\right)^2 + \left(\frac{\partial u_1}{\partial z}\right)^2\right\} + \frac{(n-1)\,(n-3)}{8}\lambda^4 \\ \left\{\left(\frac{\partial v_1}{\partial z}\right)^4 + \left(\frac{\partial u_1}{\partial z}\right)^4 + 2\left(\frac{\partial v_1}{\partial z}\frac{\partial u_1}{\partial z}\right)^2\right\} \end{array}\right]$$
$$+\eta_0 \frac{\partial v_1}{\partial z}\frac{\partial}{\partial z}$$
$$\left[\begin{array}{c} \frac{(n-1)}{2}\lambda^2 \left\{\left(\frac{\partial v_1}{\partial z}\right)^2 + \left(\frac{\partial u_1}{\partial z}\right)^2\right\} + \frac{(n-1)\,(n-3)}{8}\lambda^4 \\ \left\{\left(\frac{\partial v_1}{\partial z}\right)^4 + \left(\frac{\partial u_1}{\partial z}\right)^4 + 2\left(\frac{\partial v_1}{\partial z}\frac{\partial u_1}{\partial z}\right)^2\right\} \end{array}\right]$$
$$-\sigma B_0^2 v_1, \tag{5}$$

$$\left(u_1 \frac{\partial T}{\partial r} + w_1 \frac{\partial T}{\partial z}\right) = \alpha^* \frac{\partial^2 T}{\partial z^2}$$
$$+\tau \left[D_b \left(\frac{\partial T}{\partial z}\frac{\partial C}{\partial z}\right) + \frac{D_t}{T_\infty}\left(\frac{\partial T}{\partial z}\right)^2\right], \tag{6}$$

$$\left(u_1 \frac{\partial C}{\partial r} + w_1 \frac{\partial C}{\partial z}\right) = D_b \left(\frac{\partial^2 C}{\partial z^2}\right) + \frac{D_t}{T_\infty}\left(\frac{\partial^2 T}{\partial z^2}\right), \tag{7}$$

$$\left(u_1 \frac{\partial n}{\partial r} + w_1 \frac{\partial n}{\partial z}\right) = D_m \left(\frac{\partial^2 n}{\partial z^2}\right)$$
$$-\frac{bW_c}{\Delta C}\left(\frac{\partial}{\partial z}\left(n \frac{\partial C}{\partial z}\right)\right). \tag{8}$$

### *2.1. Boundary conditions*

The BCs subjected to fluid flow are captured as follows:

$$u_1 = u_s = l_0 r, \quad v_1 = r\Omega_1, \quad w_1 = 0,$$
$$T = T_0, \quad n = n_0, \quad C = C_0, \quad \text{at} \quad z = 0,$$
$$T \to T_\infty, \quad v_1 = u_1 \to 0, \quad n \to n_\infty,$$
$$C \to C_\infty, \quad \text{at} \quad z \to \infty. \tag{9}$$

### *2.2. Similarity analysis*

The transformations called selection of Von-Karman are expressed as follows:

$$u_1 = (\Omega_1 r)\ f(\eta), \qquad v_1 = (\Omega_1 r)\, g(\eta),$$
$$w_1 = \left(\sqrt{\nu_f \Omega_1}\right) H(\eta), \qquad \eta = \left(\sqrt{\frac{\Omega_1}{\nu_f}}\right) z,$$
$$\theta(\eta) = \frac{T - T_0}{T_0 - T_\infty}, \qquad \phi(\eta) = \frac{C - C_0}{C_0 - C_\infty},$$
$$\xi(\eta) = \frac{n - n_\infty}{n_0 - n_\infty}. \tag{10}$$

The set of dimensionless ODEs is generated as follows:

$$-(f + f) + H' = 0, \tag{11}$$

$$H''' - HH'' - \frac{1}{2}H'(H') - \frac{g^2}{2} + \frac{n-1}{2}\lambda_1 \mathrm{Re}$$
$$\left[-H''(g')g'' - H^{'''} g'^2 - H'''\frac{3}{4}H''H''\right]$$
$$+\frac{(n-3)\,(n-1)}{4(2)}\left(\lambda_1 \mathrm{Re}\right)\lambda_1 \mathrm{Re}$$
$$\left[-(g')^4 H''' - \frac{5}{16}(H'')^4 H''' - (H'')^2 \frac{3}{2} g'^2 H'''\right.$$
$$\left. -g'' 2H''(g')^3 - g''(H'')^3 g'\right] + MH' = 0, \tag{12}$$

$$g'' - g'H - H^{'} g + \lambda_1 \frac{n-1}{2}\mathrm{Re}$$
$$\left[\frac{g''H''^2}{4} + 3g'^2 g'' + g'\frac{H''}{2}H'''\right]$$
$$+\frac{(n-3)\,(n-1)}{4(2)}\left(\lambda_1 \mathrm{Re}\right)^2 \left[5g''g'^4 + \tfrac{1}{16}g''H''^4\right.$$
$$\left. +\tfrac{3}{2}H''^2 g'^2 g'' + \tfrac{g' H^{(iv)}}{4}H''^3 + \tfrac{(g')^3 H'' H'''}{4}\right] - Mg = 0, \tag{13}$$

$$\theta'' + N_b \theta' \phi' + N_t \theta'^2 - \mathrm{Pr} H\theta' = 0, \tag{14}$$

$$\phi'' + \frac{N_t}{N_b}\theta'' - Sc\phi' = 0, \tag{15}$$

$$\xi'' - Sc\xi' H + P_e\left[\phi''(\xi-\Omega)+\xi'\phi'\right]=0. \tag{16}$$

BCs regarding the flow problem are developed as follows:

$$\text{At} \quad \eta=0, \quad H=0, \quad -2St=H', \quad g=1,$$
$$\theta=1, \quad \phi=1, \quad \xi=1.$$
$$\text{At} \quad \eta\to\infty, \quad H'=0, \quad g=0, \quad \theta=0,$$
$$\phi=0, \quad \xi=0. \tag{17}$$

The influential dimensionless parameters are listed as follows:

$$\lambda_1=r^2\Omega_1^2, \quad \mathrm{Re}=\frac{r^2\Omega_1}{\nu_f}, \quad M=\frac{\sigma B_0^2}{\rho_f\Omega_1},$$
$$\mathrm{Pr}=\frac{\upsilon_f}{\alpha^*}, \quad St=\frac{l_0}{\Omega_1}, \quad N_b=\frac{D_b\tau}{\alpha^*}(C_0-C_\infty),$$
$$N_t=\frac{\tau}{\alpha^*}\frac{D_t}{T_\infty}(T_0-T_\infty), \quad \mathrm{Pe}=\frac{bW_c}{D_m},$$
$$\mathrm{Sc}=\frac{\upsilon_f}{D_m}=\frac{\upsilon_f}{D_b}, \quad \Omega=\frac{n_\infty}{(n_\infty-n_0)}. \tag{18}$$

where $\lambda_1$ is Carreau fluid, $M$ Hartmann, $N_t$ thermophoresis motion, Sc Schmidt number, $St$ stretching rate, Pr Prandtl, Re local Reynolds, Pe bio-convection Peclet, and $N_b$ Brownian motion numbers.

### 2.3. Gradient velocity and flux numbers

The gradient velocity ($C_f$), Nusselt ($\mathrm{Nu}_r$), Sherwood and motíle microorganisms ($Nn_r$) numbers are formulated as follows:

$$C_f=\frac{\sqrt{\tau_{rz}+\tau_{r\theta}}}{\rho_f(r\Omega_1)^2}, \quad \mathrm{Nu}_r=\frac{rq_1}{k(T_0-T_\infty)}, \tag{19}$$

$$\mathrm{Sh}_r=\frac{rq_2}{D_b(C_\infty-C_0)}, \quad Nn_r=\frac{rq_3}{Dm(n_\infty-n_0)}, \tag{20}$$

$$\tau_{rz}|_{z=0}=\frac{\partial u_1}{\partial z}\eta_0$$
$$\begin{bmatrix} 1+\frac{(n-1)}{2}\lambda^2\left\{\left(\frac{\partial v_1}{\partial z}\right)^2+\left(\frac{\partial u_1}{\partial z}\right)^2\right\}+ \\ \frac{(n-1)(n-3)}{8}\lambda^4\left\{\left(\frac{\partial v_1}{\partial z}\right)^4+\left(\frac{\partial u_1}{\partial z}\right)^4+2\left(\frac{\partial v_1}{\partial z}\frac{\partial u_1}{\partial z}\right)^2\right\}\end{bmatrix}, \tag{21}$$

$$\tau_{\theta z}|_{z=0}=\frac{\partial v_1}{\partial z}\eta_0$$
$$\begin{bmatrix} 1+\frac{(n-1)}{2}\lambda^2\left\{\left(\frac{\partial v_1}{\partial z}\right)^2+\left(\frac{\partial u_1}{\partial z}\right)^2\right\}+ \\ \frac{(n-1)(n-3)}{8}\lambda^4\left\{\left(\frac{\partial v_1}{\partial z}\right)^4+\left(\frac{\partial u_1}{\partial z}\right)^4+2\left(\frac{\partial v_1}{\partial z}\frac{\partial u_1}{\partial z}\right)^2\right\}\end{bmatrix}, \tag{22}$$

$$q_1=\left|-k\frac{\partial T}{\partial z}\right|_{z=0},$$

$$q_2=\left|-D_b\frac{\partial C}{\partial z}\right|_{z-0},$$

$$q_3=\left|-D_m\frac{\partial n}{\partial z}\right|_{z=0}. \tag{23}$$

Through relations, gradient velocity ($C_f$), Nusselt ($\mathrm{Nu}_{1r}$), Sherwood and motíle microorganisms ($Nn_r$) numbers resulting from the dimensionless form are as follows:

$$\mathrm{Re}^{\frac{1}{2}}(C_f)=\left(g'^2+f'^2\right)^{1/2}\left[1+\lambda_1\mathrm{Re}\left(g'g'+f'^2\right)\right]^{\frac{n-1}{2}},$$
$$\mathrm{Nu}_{1r}\mathrm{Re}^{-\frac{1}{2}}=-\theta'(0),$$
$$\mathrm{Sh}_r\mathrm{Re}^{-\frac{1}{2}}=-\phi'(0), \; Nn_r\mathrm{Re}^{-\frac{1}{2}}=-\xi'(0). \tag{24}$$

## 3. Solution analysis and physical description

The present section captures the role of fluid flow, heat energy, and mass species curves versus different parameters such as Carreau ($\lambda_1$), Hartmann ($M$), Prandtl (Pr), thermophoresis motion ($N_t$), Brownian motion ($N_b$), bioconvective Peclet (Pe), and power-law index ($n$) numbers. Figures 2–19 are sketched by applying OHAM using Mathematica 10.0. Bar charts (Figures 18–21) and numerical values in tabular forms (Tables 1–4) of different parameters are analyzed for gradient velocity ($C_f$), rate of heat energy transfer ($Nu_r$), Sherwood number ($\mathrm{Sh}_r$), and motile microorganisms ($Nn_r$).

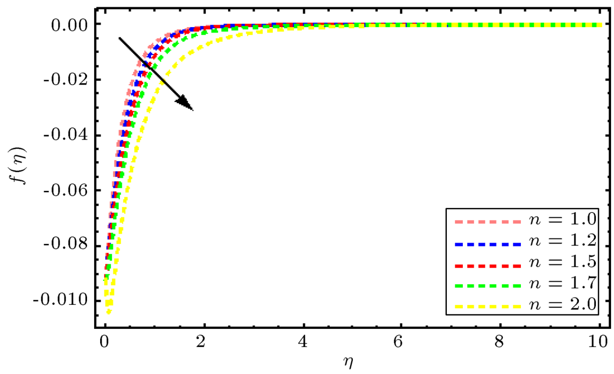


**Figure 2.** Character of $n$ regarding $f(\eta)$.

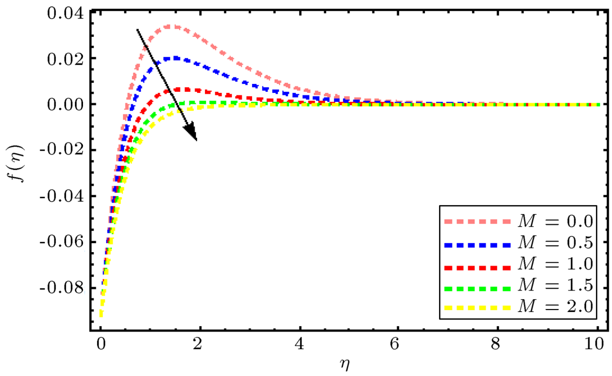


**Figure 3.** Character of $M$ regarding $f(\eta)$.

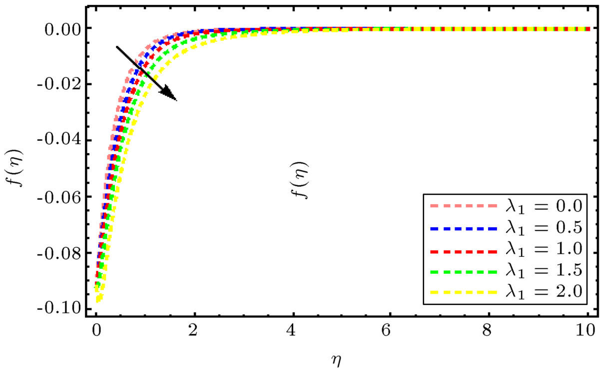


**Figure 4.** Character of $\lambda_1$ regarding $f(\eta)$.

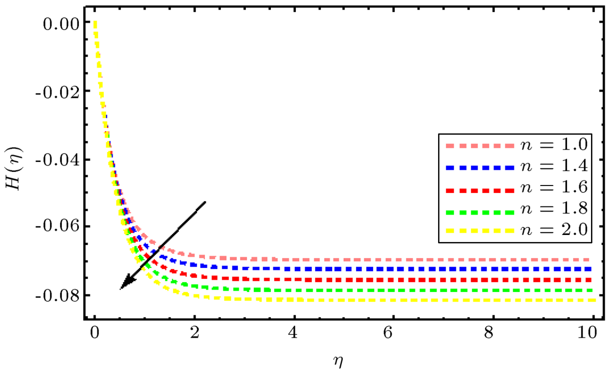


**Figure 5.** Character of $n$ regarding $H(\eta)$.

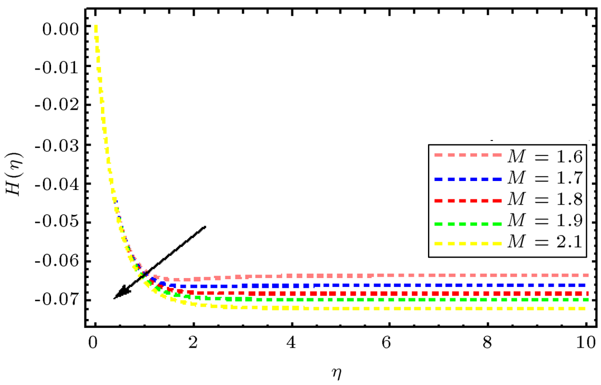


**Figure 6.** Character of $M$ regarding $H(\eta)$.

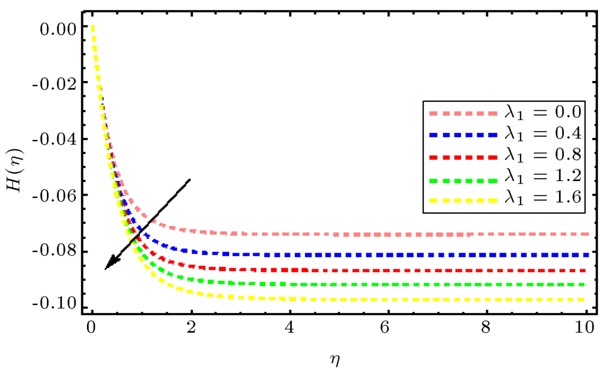


**Figure 7.** Character of $\lambda_1$ regarding $H(\eta)$.

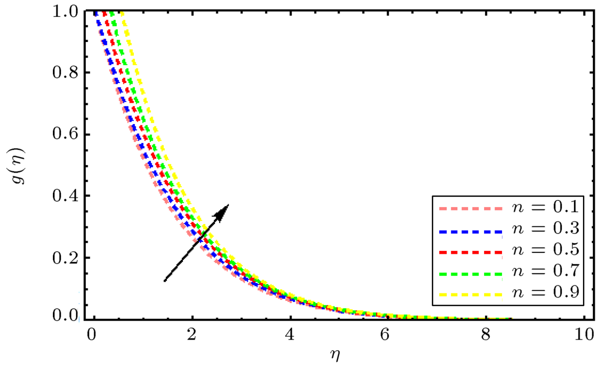


**Figure 8.** Character of $n$ regarding $g(\eta)$.

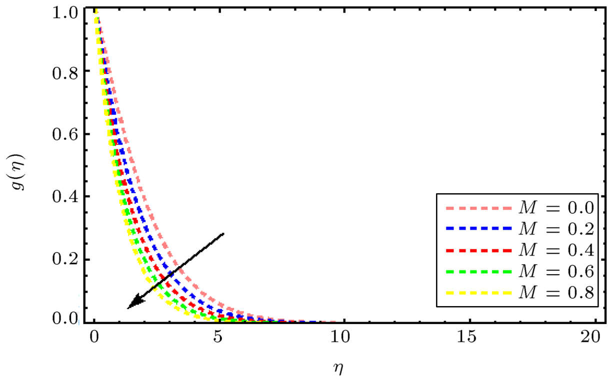


**Figure 9.** Character of $M$ regarding $g(\eta)$.

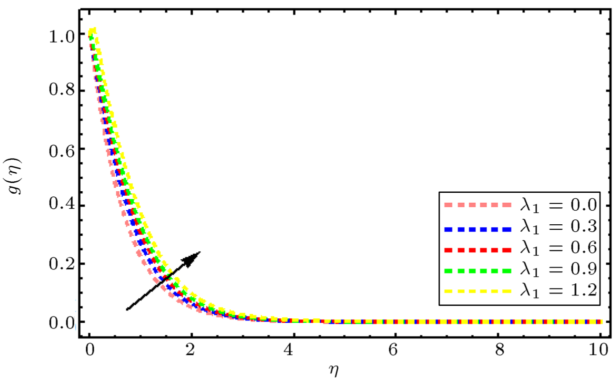


**Figure 10.** Character of $\lambda_1$ regarding $g(\eta)$.

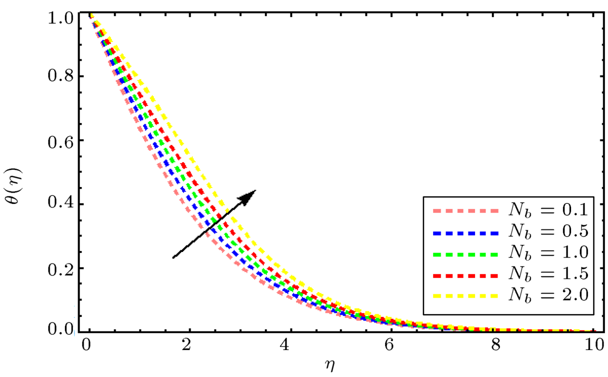


**Figure 11.** Character of $N_b$ regarding $\theta(\eta)$.

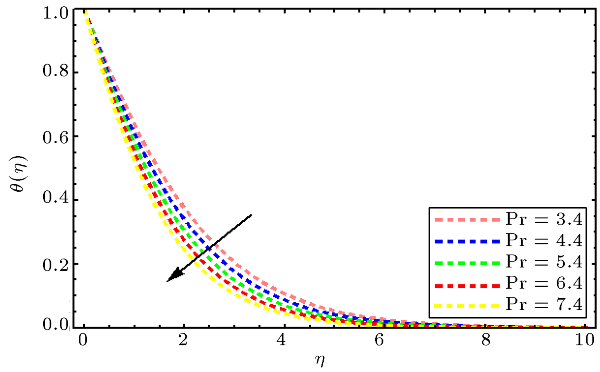


**Figure 12.** Character of Pr regarding $\theta(\eta)$.

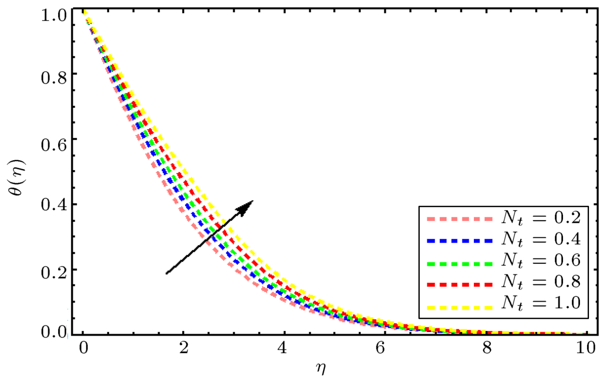


**Figure 13.** Character of $N_t$ regarding $\theta(\eta)$.

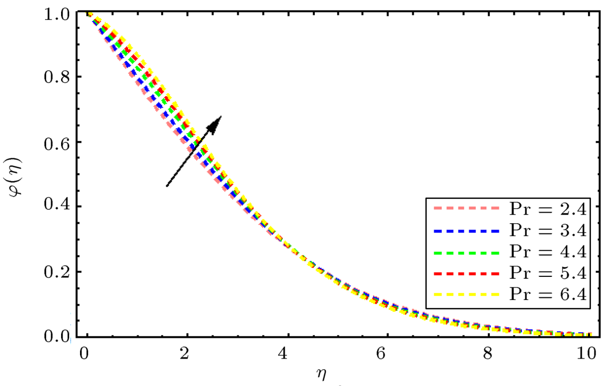


**Figure 14.** Character of Pr regarding $\varphi(\eta)$.

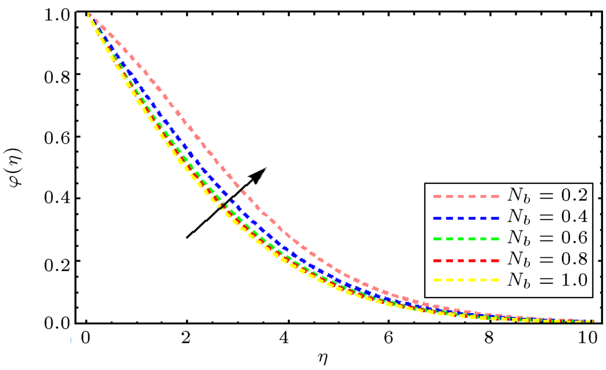


**Figure 15.** Character of $N_b$ regarding $\varphi(\eta)$.

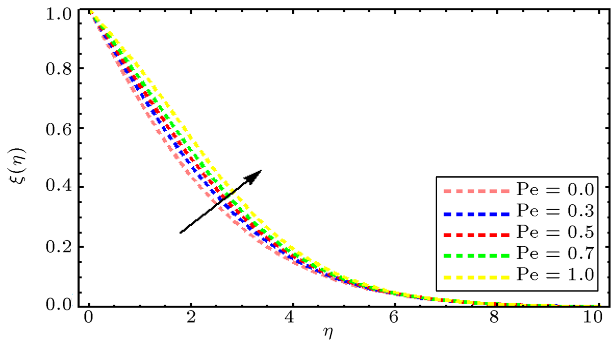


**Figure 16.** Character of Pe regarding $\xi(\eta)$.

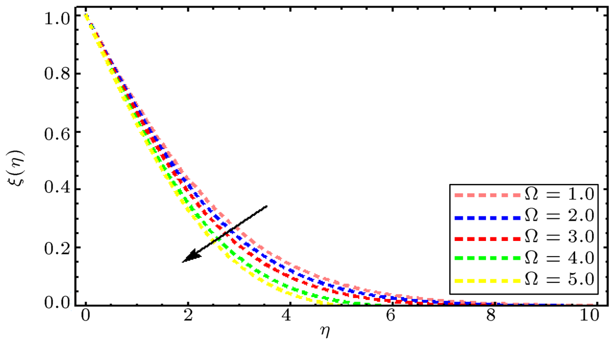


**Figure 17.** Character of $\Omega$ regarding $\xi(\eta)$.

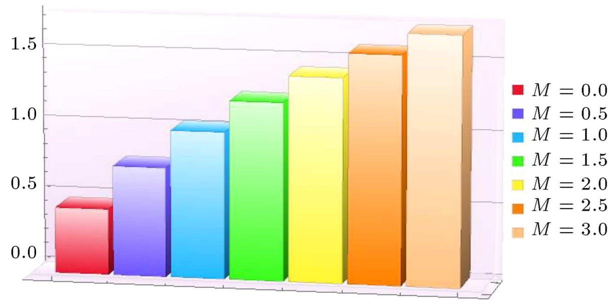


**Figure 18.** Bar chart of $C_f(\eta)$.

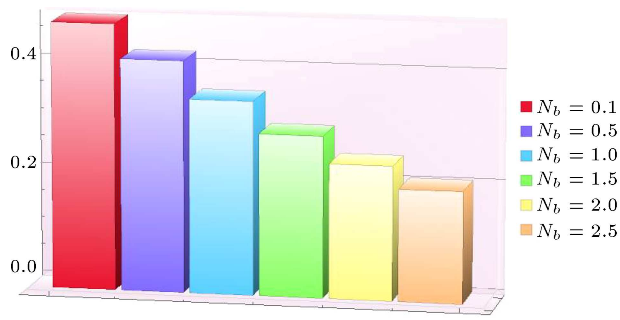


**Figure 19.** Bar chart of $\mathrm{Nu}_r(\eta)$.

The impact of $n$ on fluid flow is discussed and given in Figure 2. According to $n > 1$, the fluid acts as a shear thickening behavior since $f(\eta)$ decreases. In Figure 3, at large values of $(M)$ flow declines due to the enhancement of Lorentz force and generation of greater resistance in fluid flow particles. Similarly, Figure 4 shows the decreasing behavior for $f(\eta)$ following the


**Figure 20.** Bar chart of $Nn_r(\eta)$.

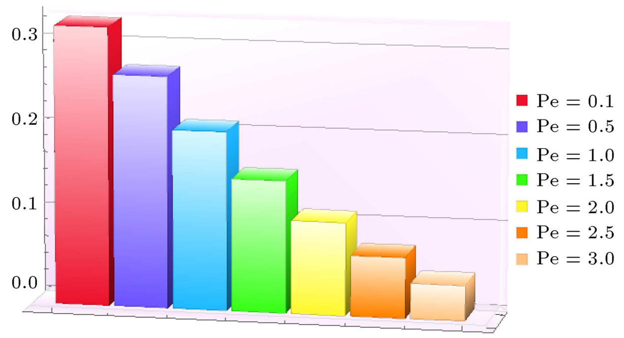


**Figure 21.** Bar chart of $Nn_r(\eta)$.

**Table 1.** Numerical values of skin friction coefficient $\mathrm{Re}^{\frac{1}{2}} C_f(0)$ when $St = 0.09$, $\lambda_1 = 0.9$, Re = 1.2, Pr = 6.7, $N_t = 0.1$, Sc = 1.2, $\Omega = 0.2$, Pe = 0.7, $N_b = 0.3$.

| $M$ | $n$ | $\lambda_1$ | Re | $\mathrm{Re}^{\frac{1}{2}} C_f$ |
|---|---|---|---|---|
| $\frac{1}{10}$ | 01 | $\frac{5}{10}$ | $\frac{9}{10}$ | 0.423187 |
| $\frac{2}{10}$ | – | – | – | 0.500069 |
| $\frac{3}{10}$ | – | – | – | 0.572402 |
| $\frac{4}{10}$ | – | – | – | 0.640583 |
| $\frac{1}{10}$ | 02 | $\frac{5}{10}$ | $\frac{9}{10}$ | 0.429413 |
| $\frac{2}{10}$ | – | – | – | 0.504486 |
| $\frac{3}{10}$ | – | – | – | 0.576577 |
| $\frac{4}{10}$ | – | – | – | 0.645889 |
| 1 | 01 | $\frac{5}{10}$ | $\frac{9}{10}$ | 0.981269 |
| $\frac{15}{10}$ | – | – | – | 1.20359 |
| 2 | – | – | – | 1.39237 |
| $\frac{25}{10}$ | – | – | – | 1.55897 |
| 1 | 02 | $\frac{5}{10}$ | $\frac{9}{10}$ | 1.01159 |
| $\frac{15}{10}$ | – | – | – | 1.26546 |
| 2 | – | – | – | 1.49019 |
| $\frac{25}{10}$ | – | – | – | 1.69825 |

escalation of Carreau parameter ($\lambda_1$). Figure 5 indicates that $H(\eta)$ velocity slows down versus large values of $n$ due to the shear thickening fluid. Similar types of behavior are given in Figure 6 against the values of $M$, while fluid particles decay because of resistive force and the motion fluid particles slow down. Figure 7 reveals

**Table 2.** Numerical study of Nusselt number $\mathrm{Re}^{-\frac{1}{2}} Nu_r$ when $n = 2.9$, $\lambda_1 = 0.9$, Re = 1.2, $\Omega = 0.2$, $M = 2.02$, Pe = 0.5, $St = 0.3$.

| $N_b$ | $N_t$ | Sc | Pr | $\mathrm{Re}^{-\frac{1}{2}}\mathrm{Nu}_r(0)$ |
|---|---|---|---|---|
| 0.1 | 0.1 | 1.0 | 6.4 | 0.480056 |
| 0.2 | – | – | – | 0.463862 |
| 0.3 | – | – | – | 0.448108 |
| 0.4 | – | – | – | 0.432789 |
| 0.1 | 0.2 | 1.0 | 6.4 | 0.467692 |
| 0.2 | – | – | – | 0.451871 |
| 0.3 | – | – | – | 0.436486 |
| 0.4 | – | – | – | 0.421534 |

**Table 3.** Numerical results with respect to Sherwood number $\mathrm{Re}^{-\frac{1}{2}}\mathrm{Sh}_r$ when $St = 0.09$, $M = 2.02$, $\lambda_1 = 0.9$, Re = 1.2, $\Omega = 0.2$, Pe = 0.7.

| $N_b$ | $N_t$ | $Sc$ | Pr | $\mathrm{Re}^{-\frac{1}{2}}\mathrm{Su}_r(0)$ |
|---|---|---|---|---|
| 0.1 | 0.1 | 1.0 | 6.4 | 0.015659 |
| 0.2 | – | – | – | –0.145346 |
| 0.3 | – | – | – | –0.198932 |
| 0.4 | – | – | – | –0.225441 |
| 0.1 | 0.2 | 1.0 | 6.4 | –0.298010 |
| 0.2 | – | – | – | –0.011591 |
| 0.3 | – | – | – | –0.114436 |
| 0.4 | – | – | – | –0.165596 |

**Table 4.** Numerical study for $\mathrm{Re}^{-\frac{1}{2}} Nn_r(0)$ when $St = 0.09$, $M = 2.02$, $\lambda_1 = 0.9$, Re = 1.2, $N_t = 0.1$, Pr = 6.7, $N_b = 0.3$.

| $P_e$ | $Sc$ | $\Omega$ | $\mathrm{Re}^{-\frac{1}{2}} Nn_r(0)$ |
|---|---|---|---|
| 0.1 | 0.5 | 0.2 | 0.32443 |
| 0.2 | – | – | 0.310349 |
| 0.3 | – | – | 0.296544 |
| 0.4 | – | – | 0.283021 |
| 0.1 | 1.0 | – | 0.340332 |
| 0.2 | – | – | 0.325989 |
| 0.3 | – | – | 0.311915 |
| 0.4 | – | – | 0.298117 |

the characteristics and effects of $\lambda_1$ on flow $H(\eta)$. It can be measured that increase in $\lambda_1$ points to the attenuation of flow phenomenon $H(\eta)$. The impact of $n$ on flow $H(\eta)$ is estimated in Figure 8. In this figure, the fluid flow is shown to be increasing for $n$ resulting from $n < 1$. The velocity of fluid $g(\eta)$ decreases due to the increasing values of intensity of $M$. According to Figure 9, it is examined that fluid flow accelerates against the large values of Carreau liquid, as can be implied from Figure 10.

Increase in the value of $N_b$ and the subsequent heat energy profile $\theta(\eta)$ outcome are given in Figure 11. It was found that heat energy curves $\theta(\eta)$ increased because of the increment of $N_b$ in fluid particle motion. Temperature profile $\theta(\eta)$ boosts up gradually due to collision between particles. Thermal Boundary Layer (TBL) is reduced upon increasing the values of Pr. Consequently, fluid temperature $\theta(\eta)$ diminishes, as can be shown in Figure 12. The temperature is enhanced because high thermophoresis parameter is $N_t$. In thermophoresis, the heat from the fluid is reduced and thermal energy increases. The effects of $N_t$ on thermal energy curves $\theta(\eta)$ are given in Figure 13. Concentration profile of nanoparticles $\varphi(\eta)$ increases due to the enhancement of momentum diffusivity. Behavior of these parameters with respect to $\varphi(\eta)$ is shown in Figure 14. Brownian motion parameter $(N_b)$ exhibits the increasing tendency of mass species profile $\varphi(\eta)$ (see Figure 15) and the concentration decreases due to the enhancement of random motion of particles and kinetic energy versus higher $N_b$. Upon increase in Pe, the speed of cells of swimming microorganisms increased. Through the pattern concentration of motile microorganisms, $\xi(\eta)$ in a moving disk increases. The graphical impact of Pe on the concentration of microorganisms $\xi(\eta)$ is depicted in Figure 16. The effect of difference in microorganism concentration on the concentration of motile microorganisms is depicted in Figure 17. To enhance the concentration difference $(\Omega)$, the concentration of motile microorganisms increases for ambient fluid and, yet, declines on the surface of $\xi(\eta)$. Figure 18 shows the bar chart for gradient velocity with different values of Hartmann number $(M)$. The figure points to the increase in values of $M$ due to high resistance between the fluid particles near the surface. Bar charts for both $\mathrm{Nu}_r$ and $\mathrm{Sh}_r$ show the opposite effect of different active values of $N_b$ according to Figures 19 and 20, respectively. To enhance the values of $N_b$ and facilitate the transport of conductive thermal energy, heat is generated due to the diffusion of nanoparticles which reduces $\mathrm{Nu}_r$ while increasing $\mathrm{Sh}_r$. Similarly, the bar chart for $Nn_r$ is plotted related to active parameter Pe in Figure 21. The numerical results regarding gradient velocity are evaluated in Table 1. According to this table, the gradient velocity reduces due to large magnetic values and enhancement of resistance to friction. Further, the rate of heat transport is reduced versus values of $(N_b)$ and $(N_t)$, whereas the rate of transport of specie sis also reduced because of $(N_b)$ and $(N_t)$ as can be observed in Table 2. Table 3 discusses the comportment of numerous influential parameters with respect to the rate of mass transportation. Table 4 exhibits the decreasing behavior of density of gyrotactic microorganisms at large values of Pe.

## 4. Key findings of performed analysis

This study investigated the transfer of thermal energy in a different light and conducted a solubility analysis for the magnetohydrodynamic flow of Carreau rheology with nanoparticles and motile microorganisms via heated disk. OHAM was applied to capture the analytic solution of fluid flow phenomenon. The characteristics of the impacts of parameters on flow, heat energy, concentration of motile microorganisms, and nanomaterial observations were conducted graphically. The valuable observation is summarized as follows:

- Increasing the values of $(n)$ had an inverse role in fluid flow due to shear thickening and shear thinning;
- Escalating values of Hartmann and Carreau fluid numbers reduced fluid flow;
- Prandtl and Brownian motion numbers had the opposite effect on fluid temperature;
- Large values of Prandtl number reduced thermal energy field and connected layer;
- The maximum heat was generated upon increasing values of thermophoresis and Brownian motion numbers;
- Enhancement of numerical values of $N_b$ results slowed down the transport of mass species;
- The transport rate for mass species also increased compared to the large values of Prandtl number;
- $\xi(\eta)$ decayed due to the difference in the concentration of microorganisms $(\Omega)$ and enhancement of Peclet number $(P_e)$;
- The gradient velocity increased as opposed to the increased values of Hartmann number;
- Large values $(N_b)$ led to a reduction in heat energy $(\mathrm{Nu}_r)$ and transport of species accelerated due to large values of $N_b$;
- Augmenting values of Peclet number reduced the density number.

## Acknowledgement

The research was supported by the National Natural Science Foundation of China (Grant Nos. 11971142, 11871202, 61673169, 11701176, 11626101, 11601485).

## References

1. Carreau, P.J. "Rheological equations from molecular network theories", *Transactions of the Society of Rheology*, **16**(1), pp. 99–127 (1972).

2. Carreau, P.J. "An analysis of the viscous behavior of polymer solutions", *Can. J. Chem. Eng.*, **57**, pp. 135–140 (1979).
3. Griffiths, P.T. "Flow of a generalised Newtonian fluid due to a rotating disk", *Journal of Non-Newtonian Fluid Mechanics*, **221**, pp. 9–17 (2015).
4. Machireddy, G.R. and Naramgari, S. "Heat and mass transfer in radiative MHD Carreau fluid with cross diffusion", *Ain Shams Engineering Journal*, **9**(4), pp. 1189–1204 (2018).
5. Kumar, K.G., Gireesha, B.J., Rudraswamy, N.G., et al. "Radiative heat transfers of Carreau fluid flow over a stretching sheet with fluid particle suspension and temperature jump", *Results in Physics*, **7**, pp. 3976–3983 (2017).
6. Irfan, M., Khan, M., and Khan, W.A. "Numerical analysis of unsteady 3D flow of Carreau nanofluid with variable thermal conductivity and heat source/sink", *Results in Physics*, **7**, pp. 3315–3324 (2017).
7. Kefayati, G.R. and Tang, H. "MHD thermosolutal natural convection and entropy generation of Carreau fluid in a heated enclosure with two inner circular cold cylinders", using LBM. *International Journal of Heat and Mass Transfer*, **126**, pp. 508–530 (2018).
8. Irfan, M., Khan, W.A., Khan, M., and Gulzar, M.M. "Influence of Arrhenius activation energy in chemically reactive radiative flow of 3D Carreau nanofluid with nonlinear mixed convection", *Journal of Physics and Chemistry of Solids*, **125**, pp. 141–152 (2019).
9. Choi, S.U.S. and Eastman, J.A. "Enhancing thermal conductivity of fluids with nanoparticles", *Presented at ASME International Mechanical Engineering Congress and Exposition* (1995).
10. Sohail, M., Naz, R., and Raza, R. "Application of double diffusion theories to Maxwell nanofluid under the appliance of thermal radiation and gyrotactic microorganism", *Multidiscipline Modeling in Materials and Structures*, **16**(2), pp. 256–280 (2020). https://doi.org/10.1108/MMMS-05-2019-0101
11. Bilal, S., Sohail, M., Naz, R., and Malik, M.Y. "Dynamical and optimal procedure to analyse the exhibition of physical attribute imparted by sutterby magneto anno fluid in darcy medium yield by axially stretched cylinder", *Canadian Journal Physics*, **98**(1), pp. 1–10 (2020).
12. Sohail, M. and Naz, R. "Modified heat and mass transmission models in the magnetohydrodynamic flow of Sutterby nanofluid in stretching cylinder", *Physica A: Statistical Mechanics and its Applications*, **549**, p. 124088 (2020).
13. Sohail, M. and Raza, R. "Analysis of radiative magneto nano pseudo-plastic material over three dimensional nonlinear stretched surface with passive control of mass flux and chemically responsive species", *Multidiscipline Modeling in Materials and Structures*, **16**(5), pp. 1061–1083 (2020).
14. Khan, H., Haneef, M., Shah, Z., Islam, S., Khan, W., and Muhammad, S. "The combined magneto hydrodynamic and electric field effect on an unsteady Maxwell nanofluid flow over a stretching surface under the influence of variable heat and thermal radiation", *Applied Sciences*, **8**(2), p. 160 (2018).
15. Sohail, M., Naz, R., and Bilal, S. "Thermal performance of an MHD radiative Oldroyd-B nanofluid by utilizing generalized models for heat and mass fluxes in the presence of bioconvective gyrotactic microorganisms and variable thermal conductivity", *Heat Transfer-Asian Research*, **48**(7), pp. 2659–2675 (2019).
16. Bhatti, M.M., Zeeshan, A., Ellahi, R., and Shit, G.C. "Mathematical modeling of heat and mass transfer effects on MHD peristaltic propulsion of two-phase flow through a Darcy-Brinkman-Forchheimer porous medium", *Advanced Powder Technology*, **29**(5), pp. 1189–1197 (2018).
17. Dogonchi, S., Alizadeh, M., and Ganji, D.D. "Investigation of MHD Go-water nanofluid flow and heat transfer in a porous channel in the presence of thermal radiation effect", *Advanced Powder Technology*, **28**(7), pp. 1815–1825 (2017).
18. Prasad, P.D., Kumar, R.V.M.S.S.K., and Varma, S.V.K. "Heat and mass transfer analysis for the MHD flow of nanofluid with radiation absorption", *Ain Shams Engineering Journal*, **9**(4), pp. 801–813 (2016).
19. Hamid, M., Usman, M., Khan, Z.H., Haq, R.U., and Wang, W. "Numerical study of unsteady MHD flow of Williamson nanofluid in a permeable channel with heat source/sink and thermal radiation", *The European Physical Journal Plus*, **133**(12), p. 527 (2018).
20. Zhao, G., Wang, Z., and Jian, Y. "Heat transfer of the MHD nanofluid in porous microtubes under the electrokinetic effects", *International Journal of Heat and Mass Transfer*, **130**, pp. 821–830 (2019).
21. Cengel, Y., *Heat and Mass Transfer: Fundamentals and Applications*, McGraw-Hill Higher Education (2020).
22. Vasilyeva, M., Babaei, M.E., Chung, T., and Spiridonov, D. "Multiscale modeling of heat and mass transfer in fractured media for enhanced geothermal systems applications", *Applied Mathematical Modelling*, **67**, pp. 159–178 (2019).
23. Vandewalle, L.A., Vijver, R.V.D., Geem, K.M.V., and Marin, G.B. "The role of mass and heat transfer in the design of novel reactors for oxidative coupling of methane", *Chemical Engineering Science*, **198**, pp. 268–289 (2019).
24. Huminic, G. and Huminic, A. "Heat transfer capability of the hybrid nanofluids for heat transfer applications", *Journal of Molecular Liquids*, **272**, pp. 857–870 (2018).
25. Karman, T.V. "Uber laminare and turbulente Reibung", *Z. Angew. Math. Mech.*, **1**, pp. 233–252 (1921).

26. Boujo, E. and Cadot, O. "Stochastic modeling of a freely rotating disk facing a uniform flow", *Journal of Fluids and Structures*, **86**, pp. 34–43 (2019).

27. Usman, M., Hamid, M., Haq, R.U., and Wang, W. "Heat and fluid flow of water and ethylene-glycol based Cu-nanoparticles between two parallel squeezing porous disks: LSGM approach", *International Journal of Heat and Mass Transfer*, **123**, pp. 888–895 (2018).

28. Lok, Y.Y., Merkin, J.H., and Pop, I. "Axisymmetric rotational stagnation-point flow impinging on a permeable stretching/shrinking rotating disk", *European Journal of Mechanics-B/Fluids*, **72**, pp. 275–292 (2018).

29. Platt, J.R. "Bioconvection patterns in cultures of free-swimming organisms", *Science*, **133**, pp. 1766–1767 (1961).

30. Chakraborty, T., Das, K., and Kundu, P.K. "Framing the impact of external magnetic field on bioconvection of a nanofluid flow containing gyrotactic microorganisms with convective boundary conditions", *Alexandria Engineering Journal*, **57**(1), pp. 61–71 (2018).

31. Khan, M., Irfan, M., and Khan, W.A. "Impact of nonlinear thermal radiation and gyrotactic microorganisms on the Magneto-Burgers nanofluid", *International Journal of Mechanical Sciences*, **130**, pp. 375–382 (2017).

32. Usman, M., Hamid, M., and Rashidi, M.M. "Gegenbauer wavelets collocation-based scheme to explore the solution of free bio-convection of nanofluid in 3D nearby stagnation point", *Neural Computing and Applications*, **31**(11), pp. 8003–8019 (2019).

33. Khan, W.A. and Makinde, O.D. "MHD nanofluid bioconvection due to gyrotactic microorganisms over a convectively heat stretching sheet", *International Journal of Thermal Sciences*, **81**, pp. 118–124 (2014).

34. Zhao, M., Xiao, Y., and Wang, S. "Linear stability of thermal-bioconvection in a suspension of gyrotactic micro-organisms", *International Journal of Heat and Mass Transfer*, **126**, pp. 95–102 (2018).

35. Marinca, V., Herişanu, N., and Nemeş, I. "Optimal homotopy asymptotic method with application to thin film flow", *Open Physics*, **6**(3), pp. 648–653 (2008).

36. Ali, L., Islam, S., Gul, T., et al. "New version of optimal homotopy asymptotic method for the solution of nonlinear boundary value problems in finite and infinite intervals", *Alexandria Engineering Journal*, **55**(3), pp. 2811–2819 (2016).

37. Bilal, S., Sohail, M., Naz, R., Malik, M.Y., and Alghamdi, M. "Upshot of ohmically dissipated Darcy-Forchheimer slip flow of magnetohydrodynamic Sutterby fluid over radiating linearly stretched surface in view of Cash and Carp method", *Applied Mathematics and Mechanics*, **40**(6), pp. 861–876 (2019).

38. Naz, R., Sohail, M., and Hayat, T. "Numerical exploration of heat and mass transport for the flow of nanofluid subject to Hall and ion slip effects", *Multidiscipline Modeling in Materials and Structures*, **16**(5), pp. 951–965 (2020).

39. Sohail, M. and Tariq, S. "Dynamical and optimal procedure to analyze the attributes of yield exhibiting material with double diffusion theories", *Multidiscipline Modeling in Materials and Structures*, **16**(3), pp. 557–580 (2019).

40. Makinde, O. and Animasaun, I. "Bioconvection in MHD nanofluid flow with nonlinear thermal radiation and quartic autocatalysis chemical reaction past an upper surface of a paraboloid of revolution", *International Journal of Thermal Sciences*, **109**, pp. 159–171 (2016).

41. Makinde, D. and Animasaun, I.L. "Thermophoresis and Brownian motion effects on MHD bioconvection of nanofluid with nonlinear thermal radiation and quartic chemical reaction past an upper horizontal surface of a paraboloid of revolution", *Journal of Molecular Liquids*, **221**, pp. 733–743 (2016).

42. Mutuku, W.N. and Makinde, O.D. "Hydromagnetic bioconvection of nanofluid over a permeable vertical plate due to gyrotactic microorganisms", *Computers & Fluids*, **95**, pp. 88–97 (2014).

43. Khan, W., Makinde, O., and Khan, Z. "MHD boundary layer flow of a nanofluid containing gyrotactic microorganisms past a vertical plate with Navier slip", *International Journal of Heat and Mass Transfer*, **74**, pp. 285–291 (2014).

44. Makinde, O.D., Kumara, B.P., Ramesh, G., and Gireesha, B.J. "Simultaneous convection of carreau fluid with radiation past a convectively heated moving plate", *Defect and Diffusion Forum*, **389**, pp. 60–70 (2018).

45. Atif, S., Hussain, S., and Sagheer, M. "Effect of thermal radiation on MHD micropolar Carreau nanofluid with viscous dissipation, Joule heating, and internal heating", *Scientia Iranica*, **26**(6), pp. 3875–3888 (2019).

46. Iqbal, M., Ghaffari, A., and Mustafa, I. "Investigation into thermophoresis and Brownian motion effects of nanoparticles on radiative heat transfer in Hiemenz flow using spectral method", *Scientia Iranica*, **26**(6), pp. 3905–3916 (2019).

47. Avinash, K., Sandeep, N., Makinde, O.D., and Animasaun, I.L. "Aligned magnetic field effect on radiative bioconvection flow past a vertical plate with thermophoresis and Brownian motion", In *Defect and Diffusion Forum*, **377**, pp. 127–140, Trans Tech Publications Ltd (2017).

## Biographies

**Muhammad Sohail** was born in a very small village of district Haripur, Khyber Pakhtunkhwa and obtained his PhD in Mathematics from the Institute of Space Technology Islamabad, Pakistan in 2020. His research interests are nanofluid, CFD, simulation, mass transport, heat transfer, MHD, Hall effect, mathematical modeling, nonlinear science, nonlinear dynamics, stability analysis, magnetrohydrodynamics, Ferro-hydrodynamic, electro-hydrodynamic, numerical and analytical methods, fractional differential equations, mixed convection, and heat exchangers. He has published about forty-seven research articles in different international journals.

**Umar Nazir** was born in an industrial city of Faisalabad, Pakistan. He did his MSc in Mathematics from GCU Faisalabad, Pakistan. Next, he completed MS (Mathematics) degree from COMSATS University, Attock, Pakistan. Then, he moved to Islamabad and completed PhD in Mathematics from Institute of Space Technology, Islamabad in February, 2021. He published about 15 research articles in different internationally reputable peer-reviewed journals. His research area is related to computational fluid dynamics, thermal stability, hybrid nanofluids, and applied mathematics.

**Yu-Ming Chu** was born in June 3, 1966, Huzhou Zhejiang, China. He received BS degree from the Hangzhou Normal University, Hangzhou, China in 1988 as well as an MS degree and PhD degree from the Hunan University, Changsha, China in 1991 and 1994, respectively. He worked as an Assistant Professor from 1994 to 1996 and as an Associate Professor from 1997 to 2002 at the Department of Mathematics, Hunan Normal University, Changsha, China. Since 2002, he has been a Professor and the Dean of the Department of Mathematics at Huzhou University, Huzhou, China. Dr. Chu's current research interests include special functions, functional analysis, numerical analysis, operator theory, ODEs, PDEs, inequalities theory and applications, and robust filtering and control.

**Wael Al-Kouz** is a Full Professor and a goal-driven, project-oriented mechanical engineer, a passionate educator, an entrepreneur, and a recognized CFD and energy expert. He enjoys seventeen years of academic research and teaching experience, with an exceptional industrial track record. Dr. Al-Kouz received his PhD in Mechanical Engineering in 2009 from Worcester Polytechnic Institute (WPI), USA. In 2013, he joined the Mechanical Engineering Department at the German Jordanian University and later served as the Head of the Department of Mechatronics Engineering during the period between 2015 and 2016. In 2016, Dr. Al-Kouz was promoted to become an Associate Professor and to a Full Professor in 2021. Currently, he is affiliated with Mechanical Engineering Department, College of Engineering, Prince Muhammad bin Fahd University, Al-Khobar, Saudi Arabia. Dr. Al-Kouz has published close to 65 articles in prestigious international journals as well as participated in numerous international conferences.

**Phatiphat Thounthong** was born in Phatthalung, Thailand, in December 1974. He received the BS and ME degrees in Electrical Engineering from the King Mongkut's Institute of Technology North Bangkok, Bangkok, Thailand in 1996 and 2001, respectively, and the PhD degree in Electrical Engineering from the Institute National Polytechnique de Lorraine University's de Lorraine, Nancy, France in 2005. Since 2012, he has been a Full Professor with the Department of Teacher Training in Electrical Engineering, King Mongkut's University of Technology North Bangkok. He has authored 105 scientific article papers published in Scopus with citations of 2,765 times and H-index of 27. His current research interests include power electronics, electric drives, electric vehicles, electrical devices (fuel cells, photovoltaic, wind turbine, batteries, and supercapacitors), nonlinear controls, and observers.